

Crosslinkable Fluorinated Hyperbranched Polyimide for Thermo-Optic Switches with High Thermal Stability

Zijian Cao,¹ Lin Jin,¹ Yu Liu,² Zhenhua Jiang,² Daming Zhang¹

¹State Key Laboratory on Integrated Optoelectronics, College of Electronic Science and Engineering, Jilin University, Changchun 130012, China

²Alan G. MacDiarmid Institute, College of Chemistry, Jilin University, Changchun, 130012, China

Correspondence to: D. Zhang (E-mail: zhangdm@jlu.edu.cn)

ABSTRACT: A series of fluorinated hyperbranched polyimides (FHBPIs) were synthesized by condensation of a triamine monomer, 1,3,5-tris(2-trifluoromethyl-4-minopheoxy) benzene (TFAPOB) and various aromatic dianhydride monomers with different linear length for application on integrated optical devices. Near infrared absorption measurement shows that it has high transparency in optical communication wavelength region. The glass transition temperature and thermal decomposition temperature were 189°C and 596°C, respectively. According to the atomic force microscopy analysis, the surface roughness of the FHBPI films is 0.208 nm. A classic Mach-Zehnder interferometer thermo-optic switch with single mode waveguide fabricated by FHBPIs represents excellent switching characteristic. The rise time and fall time of this device are 530 μs for both. © 2012 Wiley Periodicals, Inc. *J. Appl. Polym. Sci.* 000: 000–000, 2012

KEYWORDS: fluorinated polymer; hyperbranched polyimide; thermo-optic switch; Mach-Zehnder interferometer; optical waveguide

Received 11 January 2012; accepted 30 March 2012; published online

DOI: 10.1002/app.37846

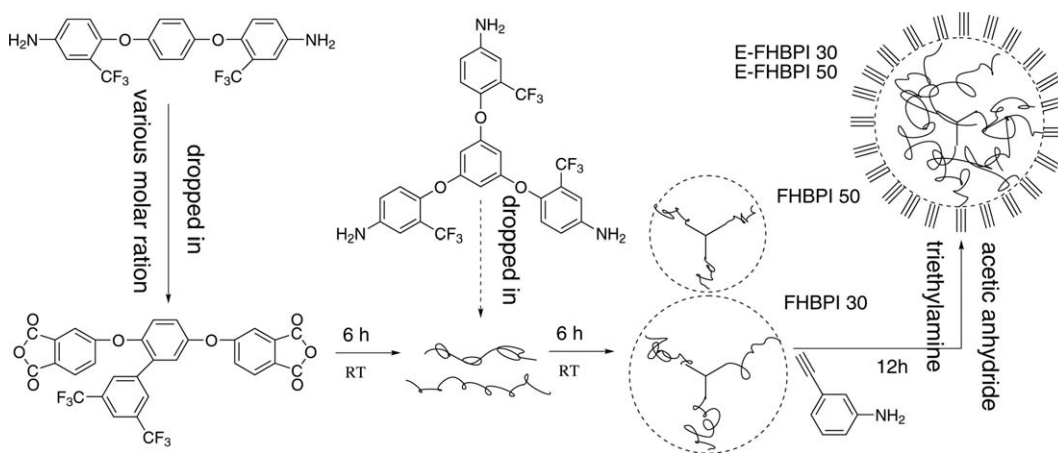
INTRODUCTION

In the past decade, polymer materials have been intensively studied for optical waveguide devices including digital optical switches, Mach-Zehnder interferometer (MZI) switches, directional coupler switches, and total-internal-reflection switches. The devices show fantastic characteristics^{1–5} such as wide bandwidth,⁶ high extinction ratio,⁷ small cubage, and easy integration. The key requirements for optical waveguide materials include low intrinsic absorption loss in the infrared communication region, high thermal and environmental stability, and flexible refractive index controllability. Compared with inorganic materials, polymer materials show attractive properties such as high thermal stability and easily controlled refractive index.^{8–10} A wide variety of polymers have been applied as optical waveguide materials, including poly(arylene ether)s,^{11,12} polyimides (PI),¹³ poly(methyl methacrylate) (PMMA),¹⁴ polystyrene (PS),¹⁵ etc. PI, an important high-performance polymer material, represents many prominent properties such as excellent thermal stability, good mechanical properties, and low coefficient of thermal expansion.^{16–20} To reduce the optical loss at infrared communication region caused by the carbon-hydrogen (C–H) bond vibrational absorption, we substitute hydrogen with heavy atoms in C–H bond, such as fluorine, deuterium,

and chlorine. Because the wavelength of the vibrational modes obtained from carbon–fluorine, carbon–deuterium, and carbon–chlorine bonds are longer than that of the vibrational mode obtained from the C–H bond,^{21–23} the absorption in optical communication region would obviously decrease. Recently, hyperbranched polymers have attracted considerable attention for their excellent properties such as low viscosity, good solubility in organic solvents, and facile fictionalization. Besides the structure researches of hyperbranched polymer, more and more studies are focused on their new applications, such as optical and electronic materials,²⁴ polymer electrolytes,²⁵ nanotechnology,²⁶ and other high-tech areas.^{27–29}

In this article, we synthesize crosslinkable fluorinated hyperbranched polyimides (FHBPIs) by condensation of a triamine monomer, 1,3,5-tris(2-trifluoromethyl-4-minopheoxy) benzene (TFAPOB), and series of aromatic ether dianhydride monomers with different flexible linear length, respectively. These FHBPIs show high optical clarity at the communication wavelength region of 1310 and 1550 nm, sufficient thermal stability, good solubility, and low birefringence, and based on these materials, high performance classic MZI thermo-optic (TO) waveguide switches are successfully fabricated, which proves that the FHBPIs could be used as suitable candidates for optical communication devices.

© 2012 Wiley Periodicals, Inc.



Scheme 1. Synthesis route of FHBPIs.

EXPERIMENTAL

Materials

FHBPIs were synthesized as shown in Scheme 1. A typical synthetic procedure of FHBPI-50 is shown as follows. Dianhydride (0.9216 g, 1.5 mmol) was dissolved in dimethylacetamide (DMAc) (10 ml) in a 100 ml three-necked flask with a nitrogen inlet.

1,4-bis(4-amino-2-trifluoromethylphenoxy)benzene (6FAPB)³⁰ (0.2142 g, 0.5 mmol) in DMAc (5 ml) was added dropwise to the dianhydride solution through a syringe. After 6FAPB solution was completely added, the reaction mixture was further stirred at room temperature for 6 h to afford an anhydride-terminated oligomer solution. Then 1,3,5-tris(2-trifluoromethyl-4-aminophenoxy)benzene (TFAPOB)⁸ (0.3017 g, 0.5 mmol) in 13 ml DMAc was added dropwise to the oligomer solution and the reaction mixture was further stirred at room temperature for 6 h to afford an anhydride-terminated hyperbranched poly(amic acid). To achieve the thermal crosslinkable FHBPI, 3-ethynylaniline was added at the end of the polymer as crosslinkable group. The poly(amic acid) was subsequently converted to PI by chemical imidization process.

To measure the refractive index and fabricate the optical waveguide, FHBPIs were dissolved in DMAc at a concentration of 10%. The solutions were filtered through a 0.2 μm Teflon membrane filter and spin-coated on silicon or silica wafer substrates. After coating, the FHBPI films were baked at 270°C for 4 h to produce 1–5 μm films.

Device Fabrication

Our proposed polymer TO switch structure is illustrated in Figure 1(a). It consists of polymer waveguides and metal heaters on the top of the upper cladding. TO waveguide switch using FHBPI-30 and FHBPI-50 polymers is fabricated following the process as described in Figure 1(b). FHBPI-30 was spin-coated onto 500 μm thick silicon as lower cladding and baked at 270°C for 4 h. Then, approximately a 4 μm thick FHBPI-50 material was spin-coated and baked at 270°C for 4 h. An aluminum (Al) film was evaporated on the FHBPI-coated wafer, as shown in Figure 1(b-1). Using photolithography, the Al film was patterned for the reactive ion etching (RIE) process in Figure 1(b-2). Then the sample was reactive ion etched for 27

min [Power: 40 W, O₂: 40 standard cubic centimeters per minute (sccm)] [Figure 1(b-3)]. After the Al mask was removed from the waveguide by chemical etching, the upper cladding FHBPI-30 was spin coated on the sample and baked. A typical cross section image of a waveguide without upper cladding is shown in Figure 2. After successfully fabricating the waveguide, we evaporated Al heaters for driving the switch. To do so, a thick metal layer was evaporated over the sample surface [Figure 1(b-4)]. By using photolithography and wet-etching, the electric heaters were fabricated and the photoresist was removed [Figure 1(b-5,6)]. A TO waveguide switch was fabricated, total length of which is 3.5 cm.

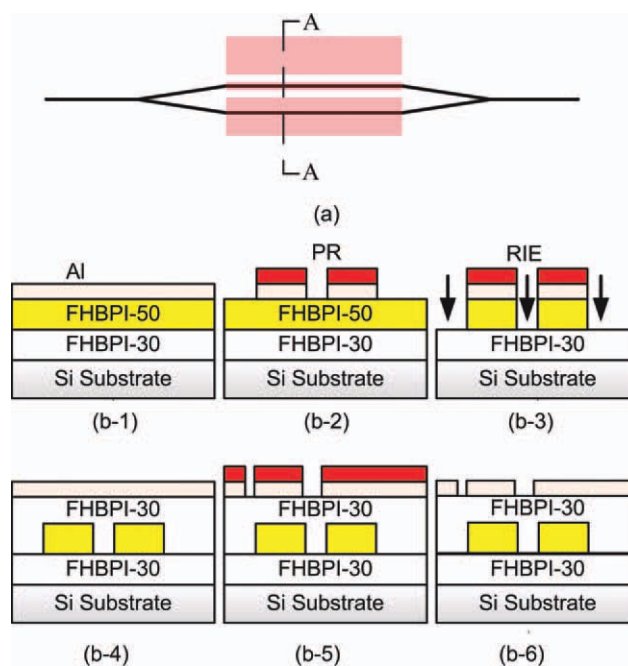


Figure 1. Proposed device model. (a) Top view of the polymer waveguide switch. (b) Fabrication process of the polymer waveguide switch. [Color figure can be viewed in the online issue, which is available at wileyonlinelibrary.com.]

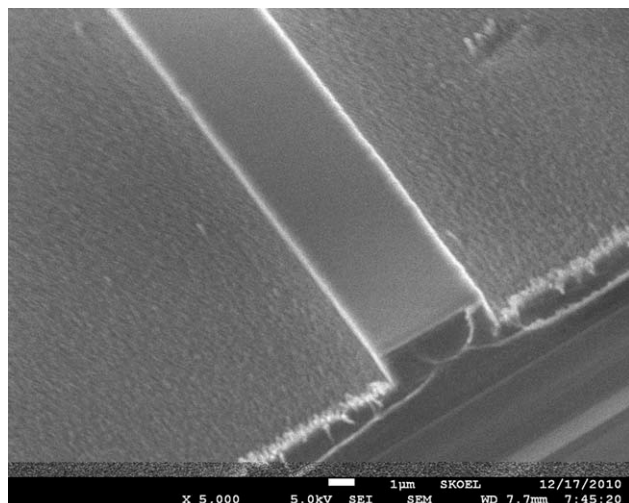


Figure 2. SEM image of the waveguide without upper cladding.

Measurements

Differential scanning calorimetry (DSC) measurement was performed on a Mettler Toledo DSC 821e instrument at a heating rate of 20°C/min under nitrogen, thermal gravimetric analyses (TGA) were determined in nitrogen atmosphere using a heating rate of 20°C/min and polymer was contained within open aluminum pans on a PERKIN ELMER TGA-7. Near infrared (NIR) absorption spectra was measured by Netzch Sta499c UV/VIS/NIR spectrophotometer. The birefringence of the film, at 650 nm wavelength, was determined by the m-lines technique for the transverse electric (TE) and transverse magnetic (TM) modes. The atomic force microscopy (AFM) observation of the surface was taken with a commercial instrument (Digital Instrument Nanoscope IIIA).

RESULTS AND DISCUSSION

Thermal Properties of FHBPI

Thermal stability is an important issue for optical component. The thermal stability of the waveguide material (FHBPI-50) was examined using by DSC and TGA. As shown in Figure 3, the glass temperature (T_g) is 189°C. Figure 4 shows the TGA curves of FHBPI-50 polymer. The thermal decomposition temperature (T_d), defined as 5% weight loss temperature, is 596°C, which is sufficiently high for optical application.

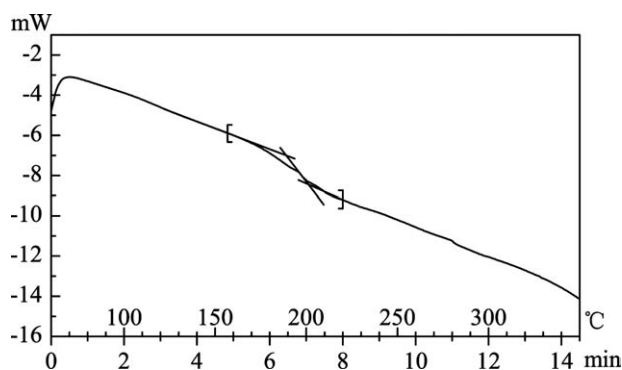


Figure 3. DSC trace of the FHBPI-50 under nitrogen at a heating rate of 20°C/min.

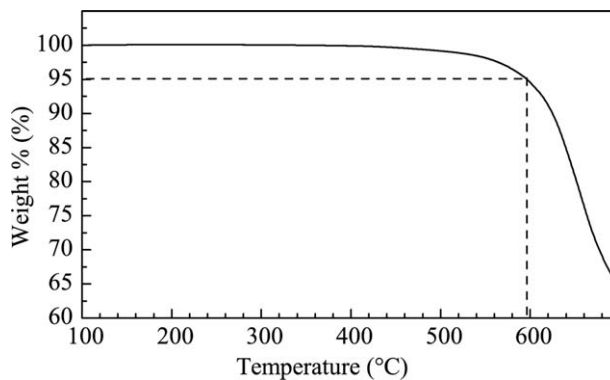


Figure 4. TGA thermogram of the FHBPI-50 under nitrogen at a heating rate of 20°C/min.

Optical Properties of FHBPI

The average refractive index (n_{AV}) estimated from the n_{TE} and n_{TM} is 1.5711. The birefringence ($\Delta n = n_{TE} - n_{TM}$) of the FHBPI-50 is 0.0065. The fact that n_{TE} value is slightly higher than the n_{TM} one for the FHBPI-50 film reflects the preferential chain orientation parallel to the film plane. It is well known that the birefringence of polymers and the internal stress σ are related by the simple equation:

$$n_{TE} - n_{TM} = C\sigma$$

where C is the stress optical coefficient. This equation indicates that the birefringence of a polymer thin film is proportional to the internal stress, which is usually caused by the spin coated, crosslinking processes, and the mismatch of coefficients of thermal expansion between film and substrate. Previous studies have demonstrated that careful control of solvent evaporation and polymer curing during film heating and cooling processes are effective in partly relieving internal stress that causes thin film optical anisotropy.³¹ But molecular design is still essential to reduce intrinsic birefringence. In FHBPI, the triamine can reduce the orientation of the bonds involved in the polymer backbone and thus reduces the birefringence, because of its non-planar and asymmetric in geometry. Based on these points, FHBPI from triamine monomer can challenge the anisotropy and low birefringence.

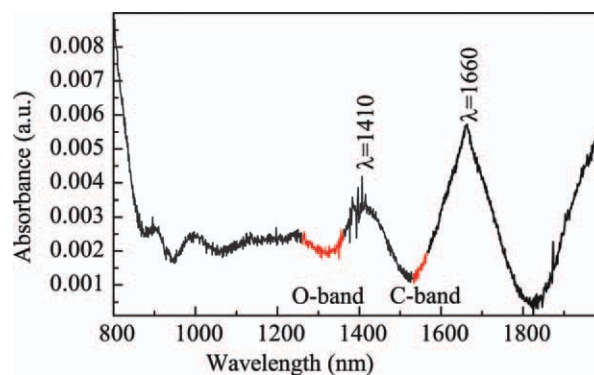


Figure 5. NIR absorption spectra of the FHBPI-50. [Color figure can be viewed in the online issue, which is available at wileyonlinelibrary.com.]

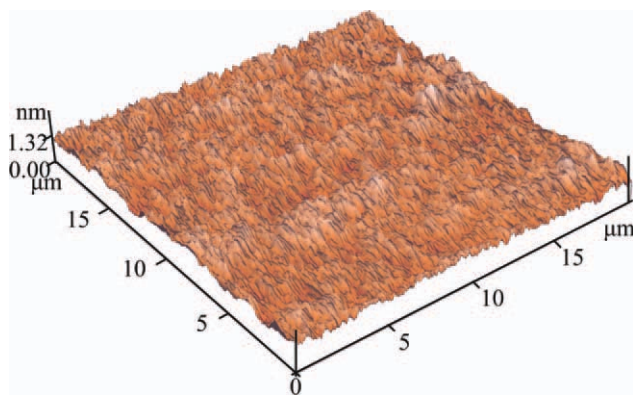


Figure 6. AFM image of FHBPI-50 film surface ($18 \times 18 \mu\text{m}^2$). [Color figure can be viewed in the online issue, which is available at wileyonlinelibrary.com.]

In the NIR region, it is known that there are three main C—H bond absorptions: (1) the C—H stretching first overtone band in the region 1600–1800 nm, (2) the combination band of the C—H stretching and deformation in the region 1330–1550 nm, and (3) the C—H stretching second overtone band in the region 1110–1200 nm.³² It has been reported that the replacement of C—H bonds with C—F bonds gives high optical transparency of the polymeric material in the NIR telecommunication region.³³ Figure 5 shows the NIR absorption spectra of the FHBPI-50. There are C—H bond vibrational absorption peak ($2\nu_{\text{C-H}}$, $\lambda = 1660 \text{ nm}$) and related peak ($2\nu_{\text{C-H}} + \delta_{\text{C-H}}$, $\lambda = 1410 \text{ nm}$) in NIR spectra of FHBPI-50. As expected, the absorption loss at 1310 and 1550 nm wavelength is very low due to the high fluorine contents.

Surface Morphology of FHBPI Film

AFM was used to study the surface roughness of FHBPI-50 film. The surface morphology of FHBPI-50 film is shown in Figure 6. The root-mean-square (RMS) surface roughness of FHBPI-50 is 0.208 nm, which is significantly smaller than the thickness of the waveguide ($4 \mu\text{m}$). Moreover, the surface roughness of the waveguide layers also relate to the scattering of the propagated light. This result shows that the FHBPI-50 is perfect for application of common waveguide device with micron scale line width.

Characteristics of MZI TO Switch

In view of the good optical properties and the excellent processability of this hyperbranched PI, it is a good candidate for waveguide material in TO waveguide switch applications. We designed and fabricated a classical MZI TO switches using FHBPI-30 and FHBPI-50 by semiconductor technology.

The performances of the device were measured as follows: The light beam (at 1550 nm) produced by a tunable semiconductor laser (TSL-210, Santec) was coupled directly into the input port by a pigtailed fiber. For optical measurement, the output light beam was collected with a lens. The near-field patterns observed by an infrared charge-coupled device (CCD) camera and displayed on a video monitor or measured by an optical power meter. A typical near-field pattern from the device at 1550 nm is shown in Figure 7(a), the optical intensity distribution of the pattern shown in Figure 7(b), which indicates that the optical waveguide of the device operates in a single mode successfully. For electrical measurements, the output light beam was collected with a photodiode as a detected signal. With microwave

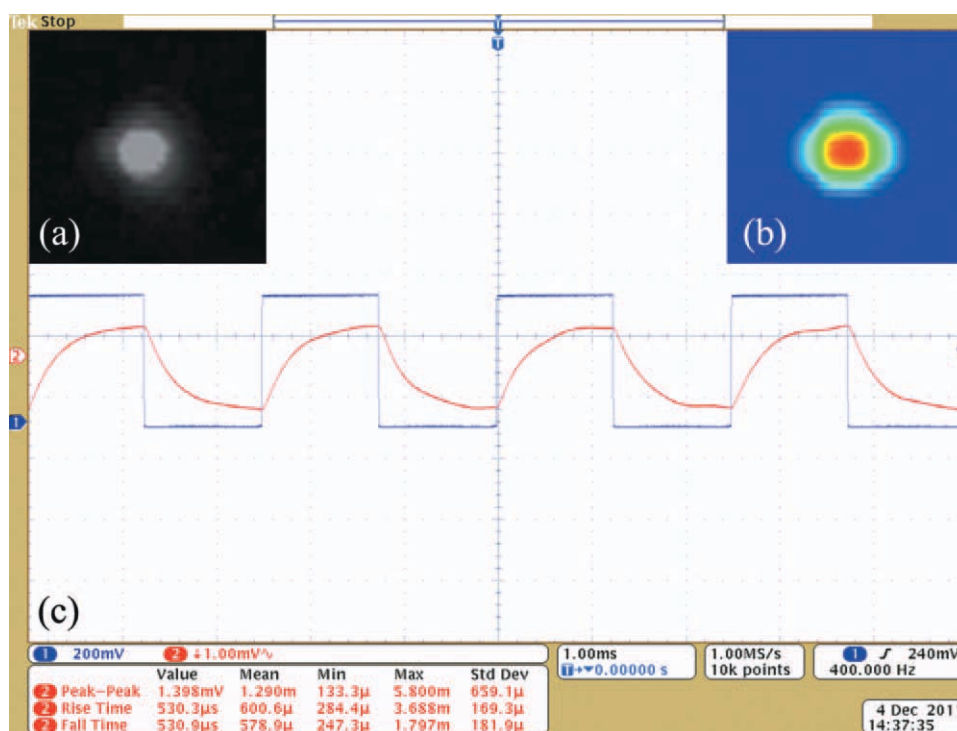


Figure 7. Switching characteristics of MZI TO switch. (a) Near-field pattern of the waveguide. (b) Optical intensity distribution of the pattern. (c) Switching characteristic of MZI TO switch. [Color figure can be viewed in the online issue, which is available at wileyonlinelibrary.com.]

probes a square wave signal is applied to the heater electrode. The driving signal and the detected signal observed on an oscilloscope (TDS2012B, Tektronix). Based on the manual of TDS2012B, the rise time is defined as the time that the leading edge of the pulse takes to rise from 10% to 90% of its amplitude. The fall time is defined as the time that the falling edge of the pulse takes to fall from 90% to 10% of its amplitude. Figure 7(c) exhibits the operational response of the switch at the wavelength of 1550 nm. The measured rise and fall time are both 530 μ s. This result indicated that the FHBPIs are good candidates for the optical switches.

CONCLUSION

Novel crosslinkable FHBPIs (FHBPI-30, FHBPI-50) were synthesized by condensation of TFAPOB and series of aromatic ether dianhydride monomers with different flexible linear length via chemical imidization technique, respectively. The thermal crosslinkable FHBPIs show a high thermal stability, good optical transparency in the infrared communication region, low birefringence, and fantastic optical property because of their special hyperbranched structures and heavy fluorine contents. Moreover, TO waveguide switch using these materials has been fabricated with excellent switching characteristic. All the characterizations proved that the FHBPIs are potential candidates for active device applications. Obviously, they can easily applied to passive devices with multilayer structure such as delay lines, array waveguide grating, and filters.

ACKNOWLEDGMENTS

This work was supported by National Natural Science Foundation of China (No. 61107019, 61177027, 61077041, and 60807029), Science Foundation for Young Scientists of Jilin Province (No. 20100174), Science and Technology Development Plan of Jilin Province (No. 20110315), and Program for Special Funds of Basic Science & Technology of Jilin University (No. 201103071, 201100253, and 200905005).

REFERENCES

- Lee, B.; Lin, C.; Wang, X.; Chen, R. T.; Luo, J.; Jen, A. K. Y. *Opt. Lett.* **2009**, *34*, 3277.
- Zheng, C.-T.; Ma, C.-S.; Yan, X.; Wang, X.-Y.; Zhang, D.-M. *J. Mod. Opt.* **2009**, *56*, 615.
- Al-Hetar, A. M.; Mohammad, A. B.; Supa'at, A.S. M.; Shamsan, Z. A.; Yulianti, I. *Opt. Commun.* **2011**, *284*, 1181.
- Oh, M. C.; Seo, J. K.; Kim, K. J.; Kim, H.; Kim, J. W.; Chu, W. S. *J. Lightwave Technol.* **2010**, *28*, 1851.
- Perron, D.; Wu, M.; Horvath, C.; Bachman, D.; Van, V. *Opt. Lett.* **2011**, *36*, 2731.
- Brosi, J. M.; Koos, C.; Andreani, L. C.; Waldow, M.; Leuthold, J.; Freude, W. *Opt. Express* **2008**, *16*, 4177.
- Deng, X. X.; Xiao, P. P.; Zheng, X.; Cao, Z. Q.; Shen, Q. S.; Zhu, K.; Li, H. G.; Wei, W.; Xie, S. X.; Zhang, Z. J. *J. Opt. A: Pure Appl. Opt.* **2008**, *10*, 1.
- Gao, H.; Wang, D.; Guan, S.; Jiang, W.; Jiang, Z.; Gao, W.; Zhang, D. *Macromol. Rapid Commun.* **2007**, *28*, 252.
- Keil, N.; Yao, H. H.; Zawadzki, C.; Strebels, B. *Electron Lett.* **1994**, *30*, 639.
- Myers, L. K.; Sakurai, Y.; Rosloniec, E. F.; Stuart, J. M.; Kang, A. H. *Am. J. Med. Sci.* **2004**, *327*, 212.
- Lee, K. S.; Kim, J. P.; Lee, J. S. *Polymer* **2010**, *51*, 632.
- Tie, W. W.; Zhong, Z. X.; Wen, P. S.; Lee, M. H.; Li, X. D. *Mater Lett.* **2009**, *63*, 1381.
- Chen, Y. C.; Chang, H. L.; Lee, R. H.; Dai, S.H. A.; Su, W. C.; Jeng, R. J. *Polym. Adv. Technol.* **2009**, *20*, 493.
- Jin, L.; Cao, Z. J.; Wang, X. B.; Ma, C. S.; Zhang, D. M. *Microw. Opt. Tech. Lett.* **2011**, *53*, 2653.
- Podzorov, A.; Gallot, G. *Appl. Opt.* **2008**, *47*, 3254.
- Chang, C. W.; Yen, H. J.; Huang, K. Y.; Yeh, J. M.; Liou, G. S. *J. Polym. Sci. Part A: Polym. Chem.* **2008**, *46*, 7937.
- Chern, Y. T.; Tsai, J. Y.; Wang, J. J. *J. Polym. Sci. Part A: Polym. Chem.* **2009**, *47*, 2443.
- Lee, G. Y.; Jang, H. N.; Lee, J. E. *J. Polym. Sci. Part A: Polym. Chem.* **2008**, *46*, 3078.
- Wang, C. Y.; Li, G.; Zhao, X. Y.; Jiang, J. M. *J. Polym. Sci. Part A: Polym. Chem.* **2009**, *47*, 3309.
- Xing, Y.; Wang, D.; Gao, H.; Jiang, Z. H. *J. Appl. Polym. Sci.* **2011**, *122*, 738.
- Louet, J. F.; Hayhurst, G.; Gonzalez, F. J.; Girard, J.; Decaux, J. F. *J. Biol. Chem.* **2002**, *277*, 37991.
- Berezhkovskiy, L. M.; Astafieva, I. V.; Cardoso, C. *Anal. Biochem.* **2002**, *308*, 239.
- Zhao, X. J.; Liu, J. G.; Li, H. S.; Fan, L.; Yang, S. Y. *J. Appl. Polym. Sci.* **2009**, *111*, 2210.
- Pitois, C.; Wiesmann, D.; Lindgren, M.; Hult, A. *Adv. Mater.* **2001**, *13*, 1483.
- Bhadra, S.; Ranganathaiah, C.; Kim, N. H.; Kim, S. I.; Lee, J. H. *J. Appl. Polym. Sci.* **2011**, *121*, 923.
- Deka, H.; Karak, N. *Polym. Adv. Technol.* **2011**, *22*, 973.
- Xie, H.; Hu, L. H.; Shi, W. F. *J. Appl. Polym. Sci.* **2012**, *123*, 1494.
- Chu, Y. J.; Xu, W. C.; Edgar, J. S.; Shou, C. Q. *J. Appl. Polym. Sci.* **2011**, *122*, 2167.
- Kelland, M. A. *J. Appl. Polym. Sci.* **2011**, *121*, 2282.
- Kreikemeyer, B.; McDevitt, D.; Podbielski, A. *Int. J. Med. Microbiol.* **2002**, *292*, 283.
- Lee, S. H.; Bae, Y. C. *Macromol. Theor. Simul.* **2000**, *9*, 281.
- Chen, H.; Yin, J. J. *J. Polym. Sci. Part A: Polym. Chem.* **2002**, *40*, 3804.
- Yen, C. T.; Chen, W. C. *Macromolecules* **2003**, *36*, 3315.